

Comparison of Capillary Architecture between Slow and Fast Muscles in Rats Using a Confocal Laser Scanning Microscope

Shinichiro Murakami^{a,b}, Hidemi Fujino^c, Isao Takeda^b,
Ryusuke Momota^a, Kanae Kumagishi^a, and Aiji Ohtsuka^{a*}

^aDepartment of Human Morphology, Okayama University Graduate School of Medicine,
Dentistry and Pharmaceutical Sciences, Okayama 700-8558, Japan,

^bDepartment of Physical Therapy, Himeji Dokkyo University, Himeji, Hyogo 670-8524, Japan, and

^cDepartment of Rehabilitation Science, Kobe University Graduate School of Health Sciences, Kobe 654-0142, Japan

The skeletal muscle is classified into 2 types, slow oxidative or fast glycolytic muscle. For further characterization, we investigated the capillary architecture in slow and fast muscles. The rat soleus and extensor digitorum longus (EDL) muscles were used as representatives of slow and fast muscles, respectively. To investigate capillary density, sections of both types of muscle were stained with alkaline phosphatase; the soleus muscle showed more intense reactivity, indicating that it had a denser capillary structure than the EDL muscle. We then injected fluorescent contrast medium into samples of both muscle types for light and confocal-laser microscopic evaluation. The capillary density and capillary-to-fiber ratio were significantly higher, and the course of the capillaries was more tortuous, in the soleus muscle than in the EDL muscle. Capillary coursed more tortuously in the soleus than in the EDL muscle. Succinate dehydrogenase (SDH) activity, an indicator of mitochondrial oxidative capacity, and vascular endothelial growth factor (VEGF) expression were also significantly higher in the soleus muscle. Thus, we conclude that slow oxidative muscle possess a rich capillary structure to provide demanded oxygen, and VEGF might be involved in the formation and/or maintenance of this highly capillarized architecture.

Key words: skeletal muscle, capillary, succinate dehydrogenase activity, vascular endothelial growth factor

Capillaries in skeletal muscle run longitudinally along muscular fibers in the resting state [1–5], and are connected by narrow anastomoses that run orthogonally to the muscle fibers [5, 6] and create an alternative circulatory route to the main longitudinal capillary. This capillary network structure is specific to skeletal muscle. Slow and fast skeletal muscles differ in function, metabolism, and blood flow characteristics [7–9]. Slow muscles have tonically active

and mainly slow-twitch fibers with an oxidative phenotype for the oxidative utilization of glucose and fatty acids, whereas fast muscles have physically active and predominantly fast-twitch fibers with a glycolytic phenotype [10].

Several studies have shown that the capillary density in mixed muscles varies with the specific type of muscle fiber being supplied by those capillaries [4]. Slow muscle fibers generally have higher capillary densities than areas containing mostly fast muscle fibers [4, 11–13]. In addition, blood flow and oxygen consumption are greater in slow muscle than in fast muscle under a resting condition [11]. However, the

influence of anastomoses on the behavior of capillary flow in muscles with different fiber compositions is poorly understood, since most studies [14–17] have evaluated only the number of capillaries per unit area of tissue, *i.e.*, the two-dimensional capillary density, and/or the numbers of capillaries per individual fiber, *i.e.*, the capillary-to-fiber (C/F) ratio, to estimate capillarity.

The purpose of the current study was to visualize three-dimensional (3-D) capillarity and to examine the net capillary volume of muscles injected with fluorescent dye using a confocal laser scanning microscope (CLSM). For this purpose, we used 2 muscles in rats, the extensor digitorum longus (EDL) and soleus muscles, as representatives of fast and slow muscles, since the former is mostly glycolytic fast muscle and the latter is purely oxidative slow [10].

Materials and Methods

Animals. All experiments were conducted in accordance with the National Institutes of Health (NIH) Guide for the Care and Use of Laboratory Animals (National Research Council, 1996) and approved by the Animal Care and Use Committee of Himeji Dokkyo University. Male Wistar rats (24–25 weeks old, $n = 8$) were used in this study. These rats were housed for 20 weeks in a room maintained under a controlled 12h light-dark cycle at a temperature of $22 \pm 2^\circ\text{C}$ with 40–60% humidity. All rats were individually housed in same-sized cages. Food and water were provided *ad libitum*.

Muscle preparation. The muscle preparation procedure was described previously [18, 19]. Briefly, animals were anesthetized with intraperitoneal administration of pentobarbital sodium (50 mg/kg). The left soleus and EDL muscles were excised and frozen in isopentane precooled in liquid nitrogen. Then, these muscles were stored at -80°C until the histochemical staining and immunoblotting analyses. After removal of the left muscles, the abdominal cavity was opened, and the left common iliac artery and vein were ligated, followed by insertion of a catheter into the abdominal aorta to keep the right hindlimb perfused with contrast medium. The right soleus and EDL muscles were first perfused for 3 min with 0.9% physiological saline containing 10,000 IU/L heparin at 37°C , followed by 10% glucose solution and the contrast

medium to be administered into the muscular circulation. The contrast medium consisted of 1% fluorescent material (PUSR80; Mitsubishi Pencil, Tokyo, Japan), 8% gelatin (Nakalai Tesque, Kyoto, Japan), and distilled water. After the perfusion with contrast medium, the whole body of the rat was quickly immersed into cold saline for 10 min. Finally, the right soleus and EDL muscles were excised and frozen in isopentane precooled in liquid nitrogen.

Histochemical procedures. The midbellies of the muscles were mounted on a specimen chuck in Tissue Tek OCT compound. Serial transverse sections ($10\mu\text{m}$ in thickness) were cut with a cryostat microtome (CM3050; Leica Microsystems, Mannheim, Germany) at -20°C , then thawed to room temperature and air-dried for 30 min. Some sections were then stained with both hematoxylin and eosin (HE) and alkaline phosphatase (AP) to visualize the capillaries in skeletal muscle. For histochemistry of alkaline phosphatase, sections were incubated in 0.1% α -naphthyl phosphate, 0.1% fast blue RR and 0.01M magnesium sulfate in 0.2M borate buffer for 60 min at 37°C , washed in distilled water and fixed with 10% formalin. Sections were observed with a light microscope ($B \times 51$; Olympus, Tokyo, Japan) and imaged with a CCD camera (VB-7000; Keyence, Osaka, Japan). The mean fiber cross-sectional area (FCSA, μm^2) from HE staining, and the capillary density and capillary-to-fiber (C/F) ratio from AP staining were calculated using NIH image software.

Some sections were also stained to determine the level of succinate dehydrogenase (SDH) activity, which is an indicator of mitochondrial oxidative capacity [20–22]. For SDH histochemistry, sections were incubated in 0.1% nitroblue tetrazolium and 0.1M sodium succinate in 0.1M phosphate buffer (pH 7.2–7.6) for 30 min at 37°C , and dehydrated through ethanol. One hundred to two hundred fibers per muscle were analyzed for the determination of SDH activity. The sectional images were visualized with a light microscope and imaged with a CCD camera. Each pixel was assigned a gray level value between 0 and 255, with the former being equivalent to 100% light transmission and the latter to 0% transmission. The mean optical density (OD) of all pixels within a fiber was determined using a calibration photographic tablet with 21 steps of gradient density ranges and the corresponding diffused density values [20–22].

3-D visualization and capillary analysis.

The 3-D capillary architecture was visualized by a fluorescent mode of confocal laser scanning microscopy (CLSM) (TCS-SP; Leica Instruments) with an argon laser (488nm), [18, 19]. In brief, the sample block was sliced into 100- μm sections using a cryostat (CM3050S; Leica Instruments). Microscopic images were obtained $\times 20$ objective lens, and each 100- μm section was scanned to a depth of 50 μm at 1 μm /slice. Microscopic observations were performed in longitudinal sections. The CLSM images were automatically rendered and displayed as 3-D images with a depth of 100 μm . Digital images were converted into stack files for morphometric analysis to a depth of 100 μm (NIH Image 1.63; NIH, Bethesda, MD, USA). The capillary volume of skeletal muscle was measured in a square with 100- μm sides and 50- μm depth by using macros included in the NIH Image software that work with stacks of 50 μm depth and [18, 19]. The microvessel volume, number of microvessels and microvessel diameter of muscular tissue were determined by measuring a $200 \times 200 \mu\text{m}^2$ area of 50 sections using NIH Image software.

Immunoblotting analysis to determine the level of vascular endothelial growth factor (VEGF). Immunoblotting analysis of the vascular endothelial growth factor (VEGF) levels was performed after homogenization of the midbelly of each muscle in an ice-cold homogenization buffer (100mM NaCl, 10mM Tris-HCl) containing protease inhibitor cocktail (P8340; Sigma Chemical, St. Louis, MO, USA). Total protein concentrations were determined using a protein assay kit (Bio-Rad Laboratories, Hercules, CA, USA) and a bovine serum albumin standard curve. To detect VEGF protein expression, each homogenized muscle sample was adjusted to a total protein content of 1 $\mu\text{g}/\mu\text{L}$. SDS-PAGE was performed using 15 μg total protein per lane for VEGF. Muscle proteins were separated on a 10–20% polyacrylamide gradient gel according to the method described by Laemmli [23]. Briefly, adjusted sample solution was added to each lane and analyzed with electrophoresis at 20mA for 1.5h at 4°C. Transfer to a PVDF membrane was achieved by the semi-dry method (100mA for 1h), followed by shaking for 1h in a 5% blocking solution (Amersham Biosciences, Piscataway, NJ, USA). The membrane was then incubated with anti-VEGF monoclonal antibody

(SC-7296; Santa Cruz, CA) for 2h. Bands were detected by chemiluminescence (ECL; Amersham Biosciences) and then photographed (LAS-3000; Fujifilm, Tokyo, Japan). Finally, the band densities were measured with image-analysis software (Science Lab; Fujifilm). Glyceraldehyde 3-phosphate dehydrogenase (GAPDH) was used in each group as an internal control.

Statistical analysis. All data are presented as the means \pm SEM. All statistical tests were made by using an unpaired Student's *t*-test. $P < 0.05$ was considered to indicate a significant difference.

Results

Muscle mass, body weight, and cross-sectional area. The body and muscle weights are summarized in Table 1. The EDL was heavier than the soleus. The fiber cross-sectional area in the EDL was significantly larger than that in the soleus muscle (Table 1).

Capillary density and SDH activity. All of the capillaries in the muscular tissue showed intense alkaline phosphatase activity, which enabled us to count them (Fig. 1). The soleus muscle possessed a high capillary density around each muscular fiber. The mean capillary density, which was determined by counting all of the capillaries in a 1mm² cross section of muscle, was significantly higher in the soleus than in the EDL muscle. The mean C/F ratio in the soleus was 148.09% of that in the EDL, and this difference was statistically significant (Fig. 1). These parameters are summarized in Table 1.

Table 1 Body and muscle parameter data in rats soleus and extensor digitorum longus muscles

	Sol	EDL	
Body mass (g)	368 \pm 6		
muscle mass (mg)	134.4 \pm 2.3	151.2 \pm 1.7	#
SDH activity (au)	100.00 \pm 1.06	82.94 \pm 0.98	#
FCSA (μm^2)	5,158 \pm 1,519	5,831 \pm 2,475	#
CD (number/mm ²)	476.24 \pm 12.04	383.06 \pm 16.29	#
C/F ratio	8.00 \pm 0.17	5.40 \pm 0.13	#

Values are means \pm S.E.M. (n = 8). Sol, soleus; EDL, extensor digitorum longus; SDH activity, succinate dehydrogenase activity; FCSA, fiber cross-sectional area; CD, capillary density; C/F ratio, capillary-to-fiber ratio.

Significantly different from sol values ($p < 0.05$).

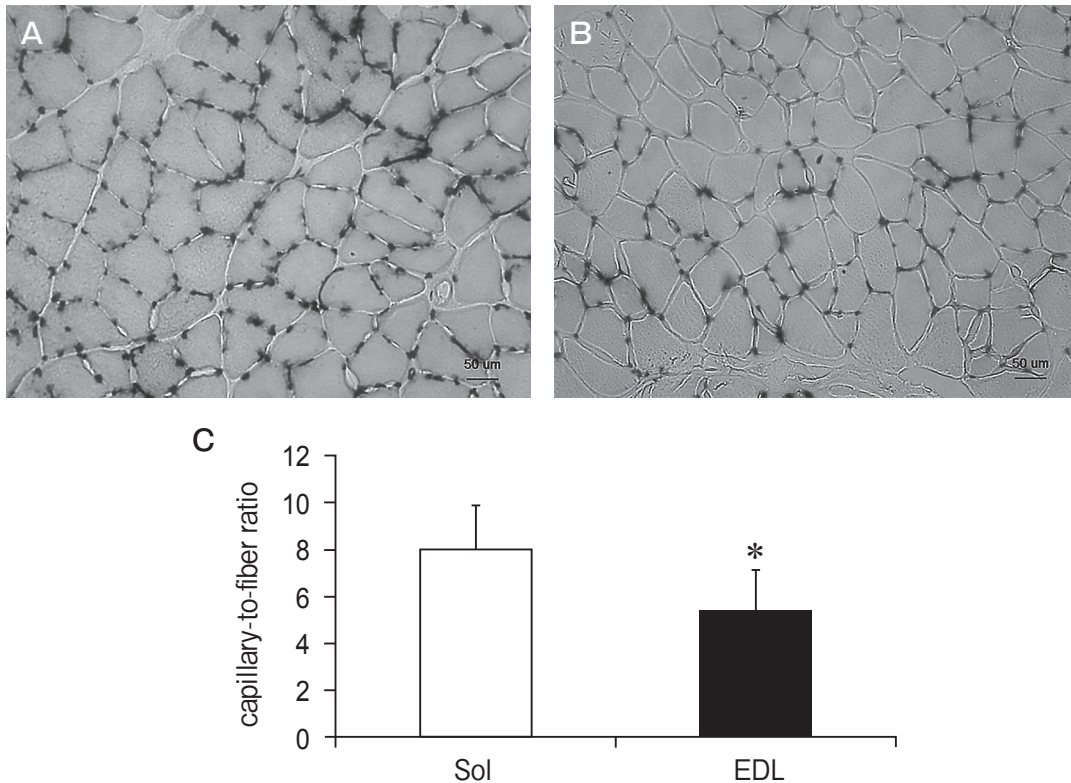


Fig. 1 Light microscopic images of capillaries and anastomoses in the soleus (A) and EDL (B) muscles, which were stained with alkaline phosphatase. The capillary-to-fiber ratio in the soleus was significantly higher than that in the EDL muscle (C). Sol, soleus; EDL, extensor digitorum longus. * $p < 0.05$. Scale bar: 50 μm .

The staining pattern for SDH activity was different between the soleus and EDL muscles (Fig. 2A, B). In the soleus, almost all of the muscle fibers showed a similar diffuse staining density for SDH activity, while in the EDL, thin fibers (approximately 50–75 μm) were stained densely, while most thick fibers (100–150 μm) showed light staining, and thus low SDH activity. The whole activity of oxidative enzyme SDH was significantly higher in the soleus than in the EDL muscle (Fig. 2, Table 1).

Capillary architecture and volume. Three-dimensionally reconstructed CLSM images revealed the capillary architecture of the soleus and EDL muscles (Fig. 3). In both muscles, longitudinal capillaries ran along the muscle fibers, and adjacent longitudinal capillaries were connected by several transverse anastomosing capillaries. The longitudinal capillaries running parallel to muscle fibers showed a tortuous course in both muscles. However, the course of the soleus muscle was more tortuous than that of

the EDL muscle, whose longitudinal capillaries waved with small amplitude.

From the morphological measurement of these CLSM images, the mean microvessel volumes of the soleus and EDL muscle were $13.57 \pm 4.04 \times 10^{-3} \text{ mm}^3/\text{mm}^3$ and $10.67 \pm 3.59 \times 10^{-3} \text{ mm}^3/\text{mm}^3$, respectively (Fig. 4). The mean microvessel volume in the soleus was significantly higher than that in the EDL muscle. Moreover, the number of capillaries and anastomoses in the soleus were $555.6 \pm 9.9/\text{mm}^2$ and $145.2 \pm 5.7/\text{mm}^2$, respectively, whereas those in the EDL muscle were $425.6 \pm 15.6/\text{mm}^2$ and $57.85 \pm 4.1/\text{mm}^2$, respectively. There was a significantly greater number of microvessels in the soleus than in the EDL muscle (Fig. 5).

The mean diameter of capillaries was $5.99 \pm 0.18 \mu\text{m}$ in the soleus muscle, and $5.11 \pm 0.17 \mu\text{m}$ in the EDL muscle. The diameter of anastomoses was $5.95 \pm 0.17 \mu\text{m}$ in the soleus and $5.76 \pm 0.22 \mu\text{m}$ in the EDL muscle. The former difference was significant, but the

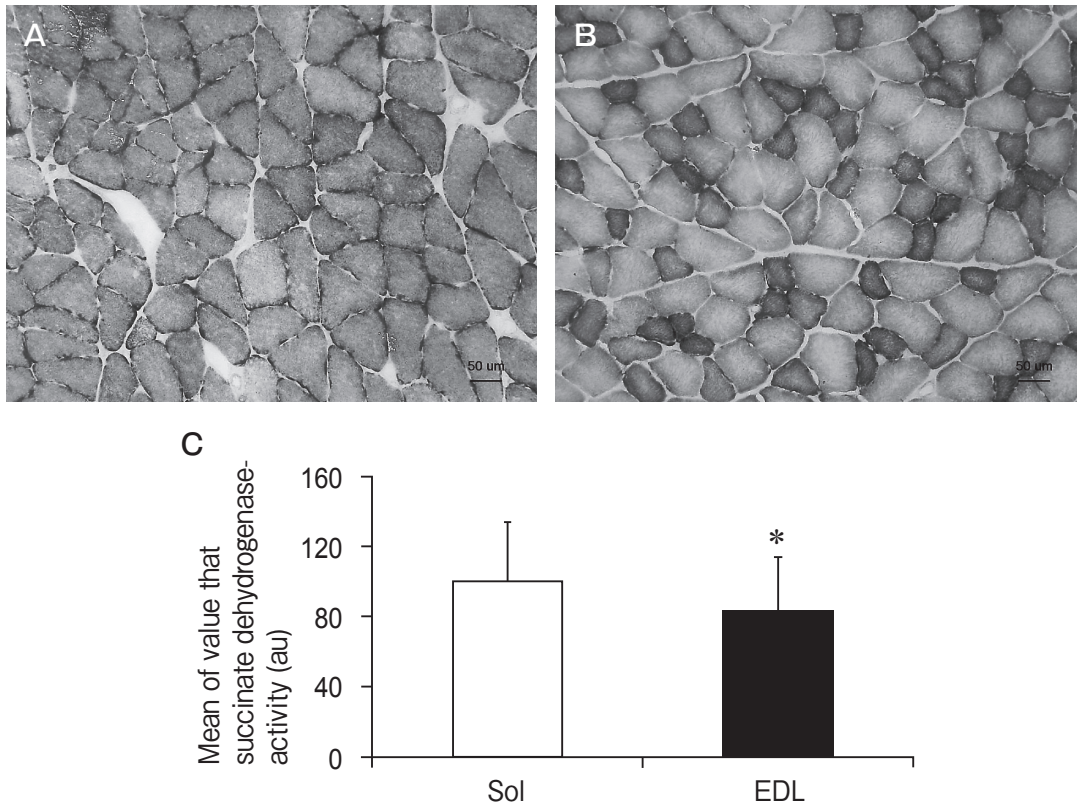


Fig. 2 Light microscopic images of capillaries and anastomoses in the soleus (A) and EDL muscles (B), which were stained for succinate dehydrogenase. The mean succinate dehydrogenase level in the soleus was significantly higher than that in the EDL muscle (C). Sol, soleus; EDL, extensor digitorum longus. * $p < 0.05$. Scale bar: 50 μm.

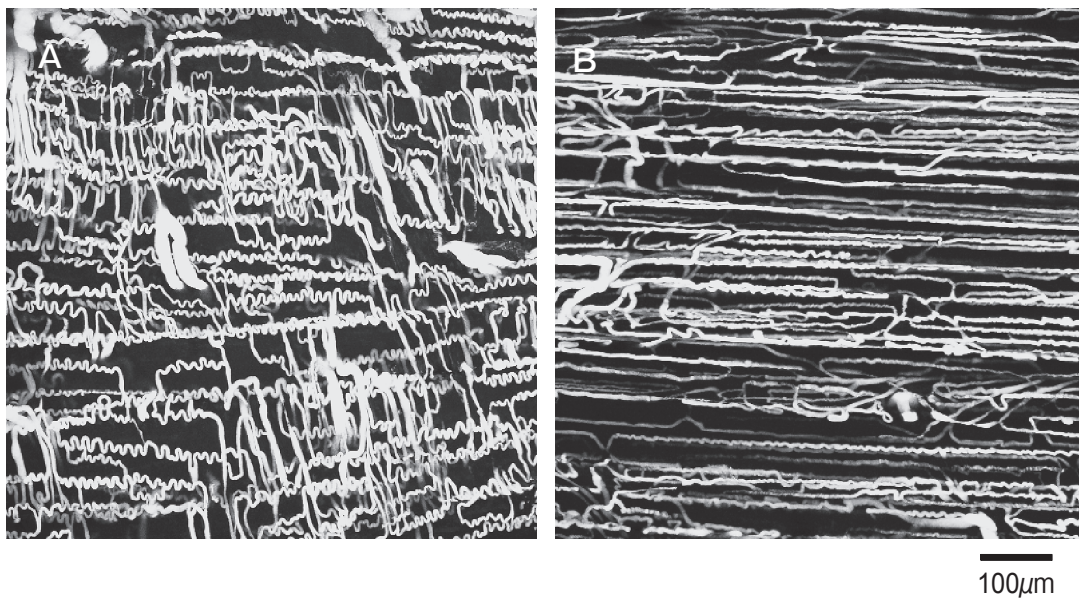


Fig. 3 Confocal laser scanning microscopic images of capillaries and anastomoses in the soleus (A) and EDL muscles (B). Capillaries run tortuously along the muscle fibers in the soleus and EDL muscle. There appear to be fewer microvessels in the EDL than the soleus muscle.

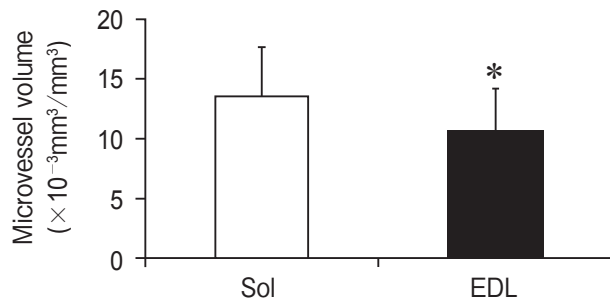


Fig. 4 The microvessel volume in the soleus was significantly higher than that in EDL muscle. Sol, soleus; EDL, extensor digitorum longus. * $p < 0.05$.

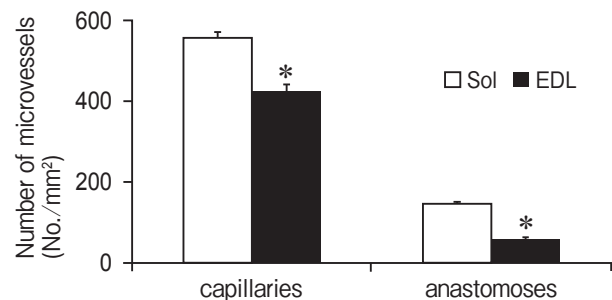


Fig. 5 The number of microvessels in the soleus was significantly higher than that in the EDL muscle. Sol, soleus; EDL, extensor digitorum longus. * $p < 0.05$.

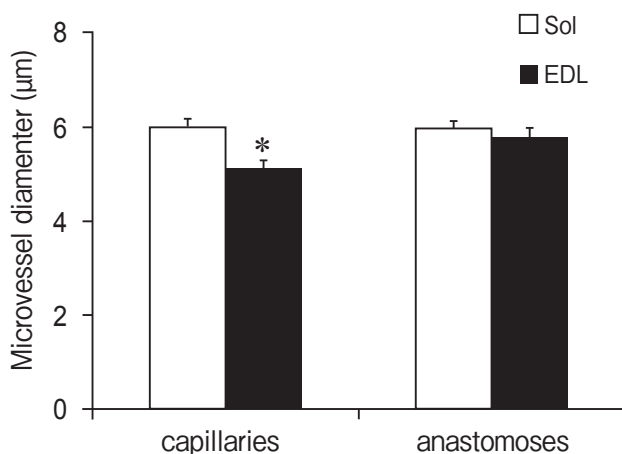


Fig. 6 The diameter of Capillaries in the soleus was significantly higher than that in the EDL muscle. However, the number of anastomoses was not significantly different between the soleus and EDL. Sol, soleus; EDL, extensor digitorum longus. * $p < 0.05$.

latter was not (Fig. 6).

VEGF expression in soleus and EDL muscles. The expression level of VEGF in the EDL muscle was 44% of that in the soleus. Thus, VEGF levels in the soleus muscle were significantly higher than those in the EDL (Fig. 7). The density of GAPDH was found to be the same in all samples.

Discussion

In the current study, the densities of the capillary network in the different 2 types of skeletal muscles were studied from stacks of perfectly registered optical images captured by a confocal laser scanning microscope. Three-dimensional methods used in this

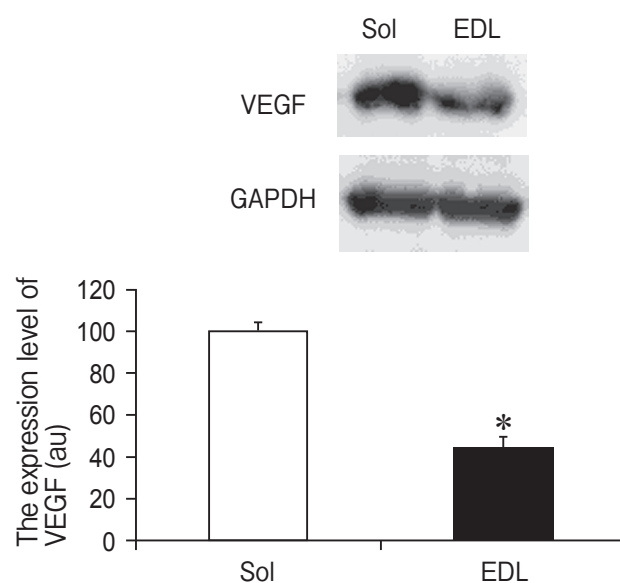


Fig. 7 The level of VEGF protein in the soleus was significantly higher than that in the EDL muscle. Sol, soleus; EDL, extensor digitorum longus. * $p < 0.05$.

study were able to correctly measure the capillary volume in the skeletal muscle, including anastomoses. The present important findings were: 1) there was a higher capillary volume in the soleus than in the EDL muscle based on CLSM images; 2) there was a higher capillary-to-fiber ratio and higher level of SDH activity in the soleus than in the EDL muscle; and 3) the level of VEGF expression was higher in the soleus than in the EDL muscle. To the best of our knowledge, this is the first report to indicate the relationship between the capillary network density and VEGF expression in rat slow and fast skeletal muscles.

Long-term unloading leads to the atrophy of skeletal muscles [11, 13, 24–26]. Atrophy occurs when contractile protein breakdown exceeds protein synthesis [24–26]. In addition, there is an increase in the proportion of the fast II_d/x isoform of myosin heavy chain in the soleus muscle (normally composed of type I and type II_a) [27–30]. This means that atrophy transforms slow-type skeletal muscles into fast-type skeletal muscles. Moreover, atrophy causes a reduction in capillary diameter and tortuosity, particularly in anastomoses, in association with vascular endothelial cell apoptosis [19]. As for microvessels, fast skeletal muscles might be less necessary than slow skeletal muscles.

The present CLMS study has shown the differences in the capillary architecture between the soleus and EDL muscles. The high capillary volume in the soleus appears to be the result of the exceedingly tortuous course of capillaries in this muscle. Myrhaage has suggested that the oxidative capacity of the fibers is more important than the fiber diameter in determining skeletal muscle capillarity [31]. Our results indicate that the differences in capillarity associated with fiber types are responsible for the differences in the capillary volume of skeletal muscle. The capillary-fiber cytoarchitecture is arranged to make the tissue more effective in meeting the demand for oxygen. The soleus muscle is an oxidative slow twitch muscle whose activity is likely to be sustained by the need to maintain posture, and it has a higher blood flow than glycolytic fast twitch muscle [9, 32]. Mai *et al.* [6] reported that the number of adjacent capillaries was greater for red type I and red type II_a fibers. Then, Poole *et al.* reported that the size of the capillary-fiber interface might be regulated in direct proportion to the fiber mitochondrial volume or maximal oxygen demand in skeletal muscles, independent of their fiber-type composition, level of aerobic capacity, degree of capillarization, and capillary geometry [14].

VEGF plays an important role in triggering angiogenesis [33]. VEGF, a 45 kDa homodimeric glycoprotein [34, 35], has been considered to be an important regulator of angiogenesis [34, 35]. In the skeletal muscle, VEGF immunohistochemical expression has been confirmed in myofibers, particularly under ischemic conditions [36]. Our results showed that VEGF expression in the soleus was higher than that in EDL

muscle. This may suggest that, when the muscles enter a hypoxic state, the VEGF in muscles induces an increase in the number of blood vessels. In the case of EDL, mostly glycolytic fast muscle requires less oxygen supply from the blood vessels, so that the VEGF expression might be lower than in the soleus. Thus, the capillary volume and VEGF expression in slow muscles such as the soleus are much higher than those in fast muscles such as the EDL.

Most previous studies [14–16] have used the number of capillaries per unit area of tissue, *i.e.*, two-dimensional capillary density, and/or the numbers of capillaries per individual fiber, *i.e.*, capillary-to-fiber ratio, to estimate capillarity. In contrast, 2 recent studies determined the three-dimensional architecture of muscle capillary by CLMS, and the real capillary volume per unit cubage of tissue in heart and skeletal tissues [18, 19]. We used these 2 techniques in the present study, and we found a significantly higher capillary volume in the soleus muscle than that in the EDL muscle, which was not surprising, since soleus muscle has the higher oxidative capacity. In the present study, capillaries of the soleus showed an extraordinarily tortuous course. Such tortuosity should be distinguished from the results regarding the contractile position. The current comparison of capillarity between the 2 muscles was done under a no-load condition by removing the muscles. In conclusion, our study revealed differences in capillarity, especially anastomosis, and capillary volume *ex vivo* between the soleus and EDL muscles of rats. The capillary volume and VEGF expression in slow muscle were found to be higher than those in fast muscle. These findings suggest that differences in the capillary architecture between slow and fast muscles may have arisen in order to meet the different levels of oxygen demand.

Acknowledgments. This study was supported by Grants-in-Aid for Scientific Research (19300196 and 21700559) from the Japanese Ministry of Education, Culture, Sports, Science and Technology.

References

1. Batra S and Rakusan K: Capillary length, tortuosity, and spacing in rat myocardium during cardiac cycle. *Am J Physiol Heart Circ Physiol* (1992) 263: H1369–H1376.
2. Dawson JM, Tyler KR and Hudlicka O: A comparison of the microcirculation in rat fast glycolytic and slow oxidative muscles at rest and during contractions. *Microvasc Res* (1987) 33: 167–182.

3. Mathieu-Costello O: Capillary tortuosity and degree of contraction or extension of skeletal muscles. *Microvasc Res* (1987) 33: 98–117.
4. Mathieu-Costello O, Ellis CG, Potter RF, MacDonald IC and Groom AC: Muscle capillary-to-fiber perimeter ratio: morphometry. *Am J Physiol Heart Circ Physiol* (1991) 261: H1617–H1625.
5. Wiedeman MP: Patterns of the arterovenous pathways; in *Handbook of Physiology, Circulation*, Washington DC, Am Physiol Soc, 1963, sect. 2, vol. II, pp 891–933.
6. Mai JV, Edgerton VR and Barnard RJ: Capillarity of red, white and intermediate muscle fibers in trained and untrained guinea pigs. *Experientia* (1970) 26: 1222–1223.
7. Schmidt-Nielsen K and Pennycuik P: Capillary density in mammals in relation to body size and oxygen consumption. *Am J Physiol* (1961) 200: 746–750.
8. Deveci D, Marshall JM and Egginton S: Relationship between capillary angiogenesis, fiber type, and fiber size in chronic systemic hypoxia. *Am J Physiol Heart Circ Physiol* (2001) 281: H241–H252.
9. Hudlicka O, Brown M and Egginton S: Angiogenesis in skeletal and cardiac muscle. *Physiol Rev* (1992) 72: 369–417.
10. Delp MD and Duan C: Composition and size of type I, IIA, IID/X, and IIB fibers and citrate synthase activity of rat muscle. *J Appl Physiol* (1996) 80: 261–270.
11. McDonald KS, Delp MD and Fitts RH: Effect of hindlimb unweighting on tissue blood flow in the rat. *J Appl Physiol* (1992) 72: 2210–2218.
12. Desplanches D, Kayar SR, Sempore B, Flandrois R and Hoppeler H: Rat soleus muscle ultrastructure after hindlimb suspension. *J Appl Physiol* (1990) 69: 504–508.
13. Morey ER: Spaceflight and bone turnover: correlation with a new rat model of weightlessness. *Bioscience* (1979) 29: 168–172.
14. Poole DC and Mathieu-Costello O: Relationship between fiber capillarization and mitochondrial volume density in control and trained rat soleus and plantaris muscles. *Microcirculation* (1996) 3: 175–186.
15. Deveci D, Marshall JM and Egginton S: Relationship between capillary angiogenesis, fiber type, and fiber size in chronic systemic hypoxia. *Am J Physiol Heart Circ Physiol* (2001) 281: H241–H252.
16. Mathieu-Costello O, Agey PJ, Wu L, Hang J and Adair TH: Capillary-to-fiber surface ratio in rat fast-twitch hindlimb muscles after chronic electrical stimulation. *J Appl Physiol* (1996) 80: 904–909.
17. Kano Y, Shimegi S, Takahashi H, Masuda K and Katsuta S: Changes in capillary luminal diameter in rat soleus muscle after hind-limb suspension. *Acta Physiol Scand* (2000) 169: 271–276.
18. Toyota E, Fujimoto K, Ogasawara Y, Kajita T, Shigeto F, Matsumoto T, Goto M and Kajiji F: Dynamic changes in three-dimensional architecture and vascular volume of transmural coronary microvasculature between diastolic- and systolic-arrested rat hearts. *Circulation* (2002) 105: 621–626.
19. Fujino H, Kohzuki H, Takeda, Kiyooka T, Miyasaka T, Mohri S, Shimizu J and Kajiji F: Regression of capillary network in atrophied soleus muscle induced by hindlimb unweighting. *J Appl Physiol* (2005) 98: 1407–1413.
20. Wüst RC, Gibbings SL and Degens H: Fiber capillary supply related to fiber size and oxidative capacity in human and rat skeletal muscle. *Adv Exp Med Biol* (2009) 645: 75–80.
21. Esteva S, Panisello P, Casas M, Torrella JR, Pagés T and Viscor G: Morphofunctional responses to anaemia in rat skeletal muscle. *J Anat* (2008) 212: 836–844.
22. Biring MS, Fournier M, Ross DJ and Lewis MI: Cellular adaptations of skeletal muscles to cyclosporine. *J Appl Physiol* (1998) 84: 1967–1975.
23. Laemmli UK: Cleavage of structural proteins during the assembly of the head of bacteriophage T4. *Nature* (1970) 227: 680–685.
24. Thomason DB, Biggs RB and Booth FW: Protein metabolism and beta-myosin heavy-chain mRNA in unweighted soleus muscle. *Am J Physiol* (1989) 257: R300–R305.
25. Thomason DB and Booth FW: Atrophy of the soleus muscle by hindlimb unweighting. *J Appl Physiol* (1990) 68: 1–12.
26. Jackman RW and Kandarian SC: The molecular basis of skeletal muscle atrophy. *Am J Physiol Cell Physiol* (2004) 287: C834–C843.
27. Takahashi H, Wada M and Katsuta S: Expressions of myosin heavy chain IId isoform in rat soleus muscle during hindlimb suspension. *Acta Physiol Scand* (1991) 143: 131–132.
28. Campione M, Ausoni S, Guezennec CY and Schiaffino S: Myosin and troponin changes in rat soleus muscle after hindlimb suspension. *J Appl Physiol* (1993) 74: 1156–1160.
29. Adams GR, Haddad F and Baldwin KM: Interaction of chronic creatine depletion and muscle unloading: effects on postural locomotor muscles. *J Appl Physiol* (1994) 77: 1198–1205.
30. Fauteck SP and Kandarian SC: Sensitive detection of myosin-heavy chain composition in skeletal muscle under different loading conditions. *Am J Physiol* (1995) 268: C419–C424.
31. Myrhaeghe R: Capillary supply of the muscle fibre population in hindlimb muscles of the cat. *Acta Physiol Scand* (1978) 103: 19–30.
32. Williams DA and Segal SS: Microvascular architecture in rat soleus and extensor digitorum longus muscles. *Microvasc Res* (1992) 43: 192–204.
33. Suzuki J: Time-course changes in VEGF expression and capillarity in the early stage of exercise training with Co treatment in rat skeletal muscles. *Acta Physiol Scand* (2004) 181: 225–232.
34. Amaral SL, Papanek PE and Greene AS: Angiotensin II and VEGF are involved in angiogenesis induced by short-term exercise training. *Am J Physiol Heart Circ Physiol* (2001) 281: H1163–H1169.
35. Richardson RS, Wagner H, Mudaliar SRD, Henry R, Noyszewski EA and Wagner PD: Human VEGF gene expression in skeletal muscle: effect of acute normoxic and hypoxic exercise. *Am J Physiol Heart Circ Physiol* (1999) 277: H2247–H2252.
36. van Weel V, Seghers L, de Vries MR, Kuiper EJ, Schlingemann RO, Bajema IM, Lindeman JH, Delis-van Diemen PM, van Hinsbergh VW, van Bockel JH and Quax PH: Expression of vascular endothelial growth factor, stromal cell-derived factor-1, and CXCR4 in human limb muscle with acute and chronic ischemia. *Arterioscler Thromb Vasc Biol* (2007) 27: 1426–1432.